Electronic Supplementary Material (ESI) for New Journal of Chemistry.


# SUPPORTING INFORMATION

# Step by step designing of sensitive luminescent nanothermometers based on $Cr^{3+}$,$Nd^{3+}$ co-doped $La_{3-x}$ $Lu_xAl_{5-y}Ga_yO_{12}$ nanocrystals

**K. Elzbieciak-Piecka[1], C. Matuszewska[1] L. Marciniak[1*]**

[1] *Institute of Low Temperatures and Structure Research PAS*

***e-mail l.marciniak@intibs.pl**

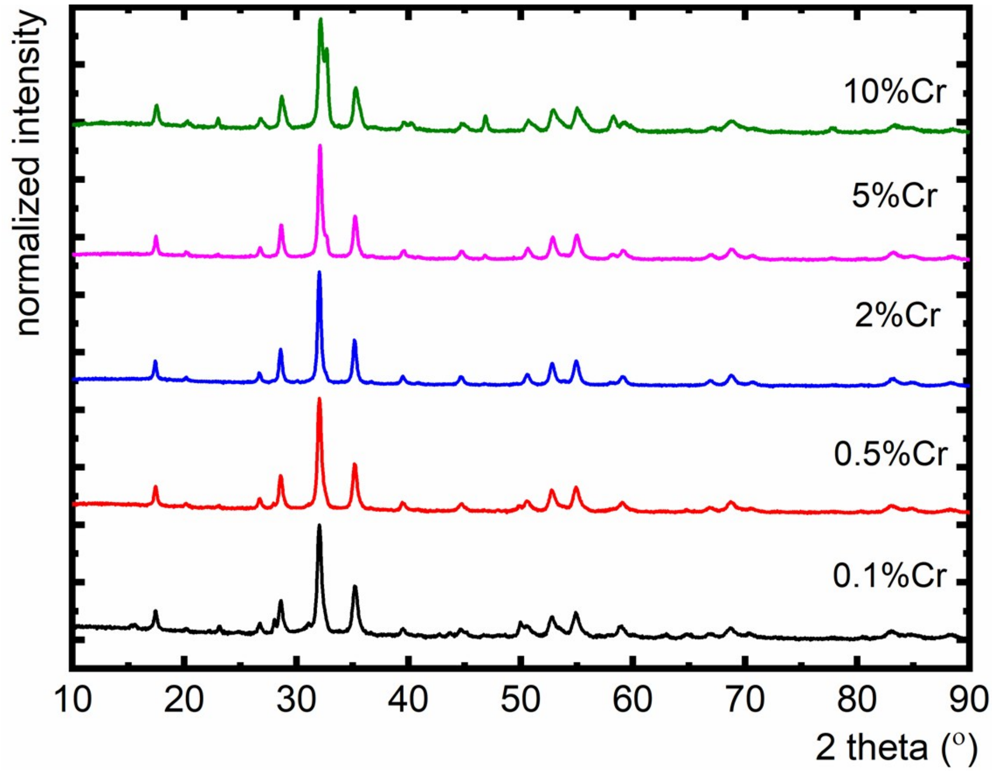


**Figure S.1.** XRD patterns for $La_2LuGa_5O_{12}$: $Cr^{3+}$ with different concentrations of $Cr^{3+}$ dopant.

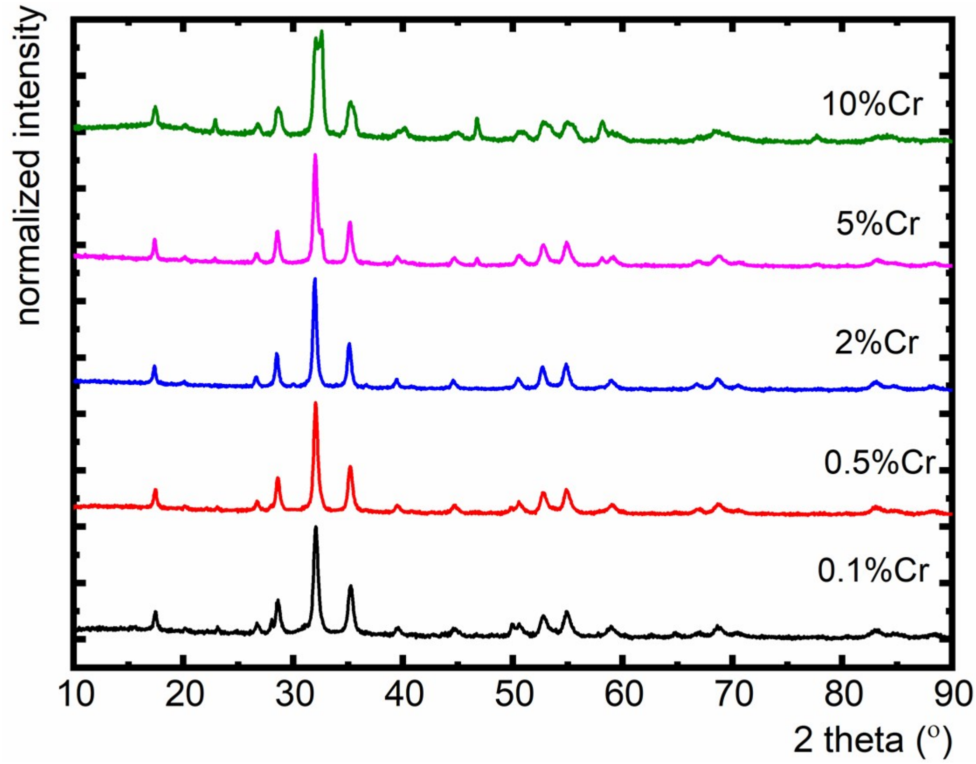


**Figure S.2.** XRD patterns for $La_2LuGa_5O_{12}$: $Cr^{3+}$, 1%$Nd^{3+}$ with different concentrations of $Cr^{3+}$ dopant.

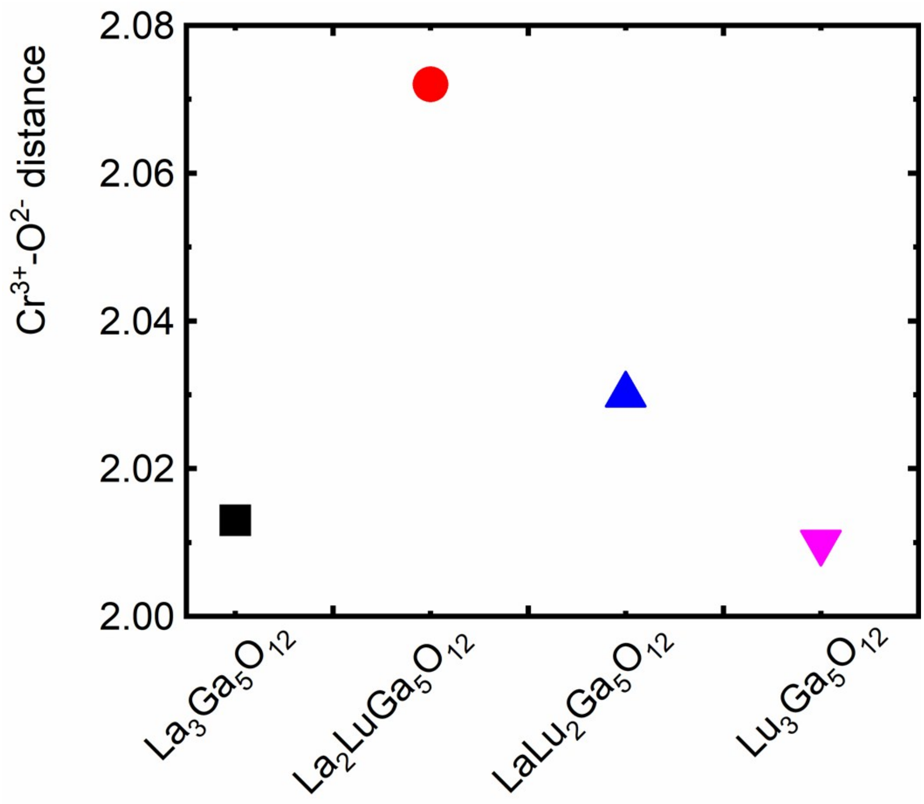


**Figure S.3.** $Cr^{3+}$-$O^{2-}$ ionic distances in $La_{3-x}Lu_xGa_5O_{12}$: 1%$Cr^{3+}$.

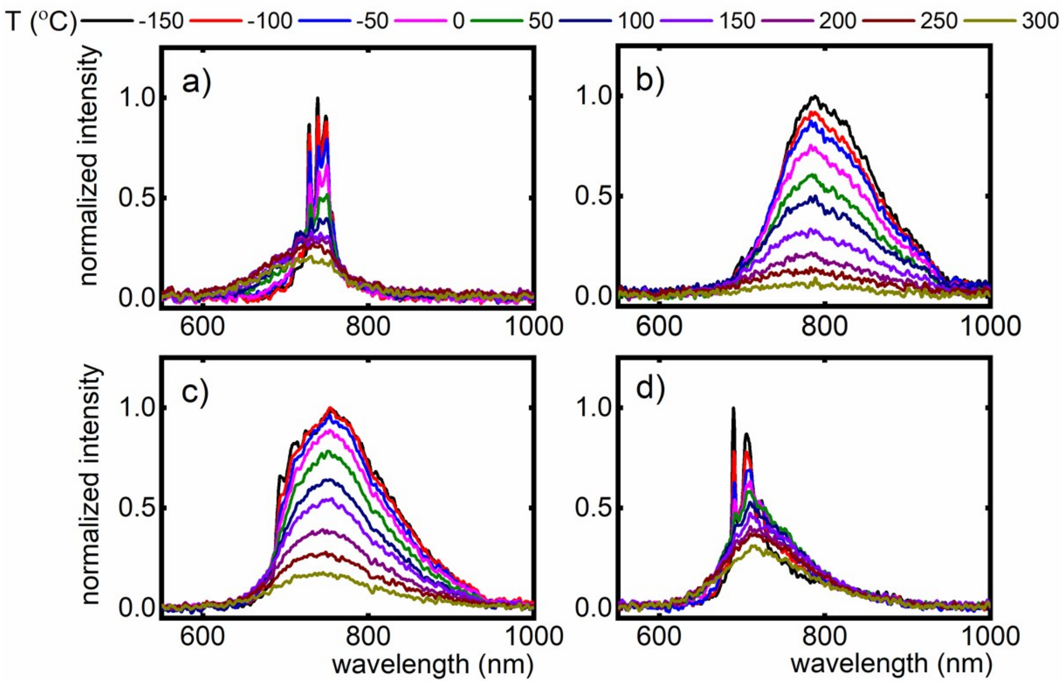


**Figure S.4.** Comparison of $La_{3-x}Lu_xGa_5O_{12}$: 1%$Cr^{3+}$ emission spectra in the function of temperature: $La_3Ga_5O_{12}$ –a); $La_2LuGa_5O_{12}$ –b); $LaLu_2Ga_5O_{12}$ –c); $Lu_3Ga_5O_{12}$ –d).

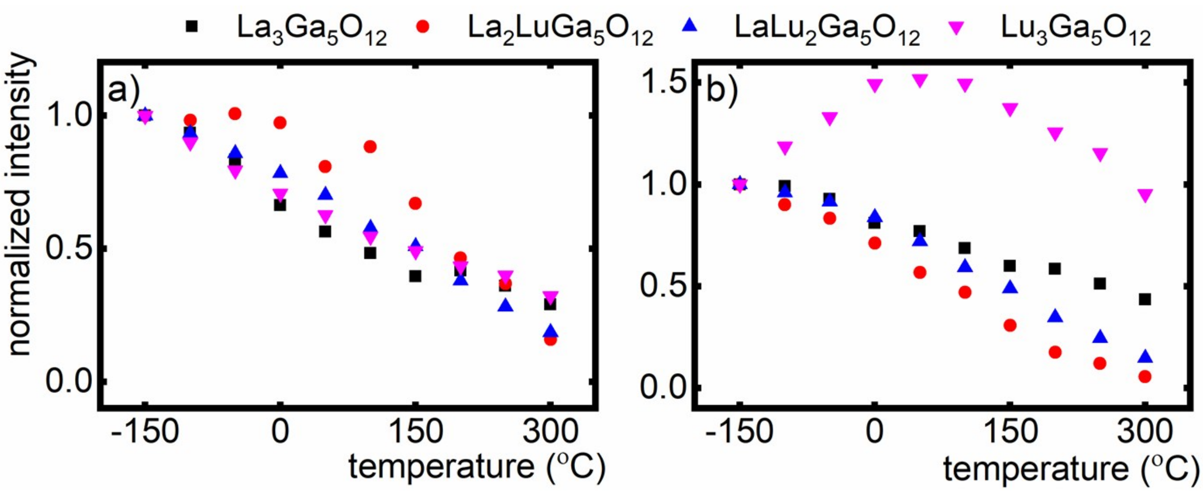


**Figure S.5.** Integral intensity of $^2E \rightarrow {}^4A_2$ -a) and $^4T_2 \rightarrow {}^4A_2$ -b) electronic transitions in the function of temperature for $La_{3-x}Lu_xGa_5O_{12}$: 1%$Cr^{3+}$.

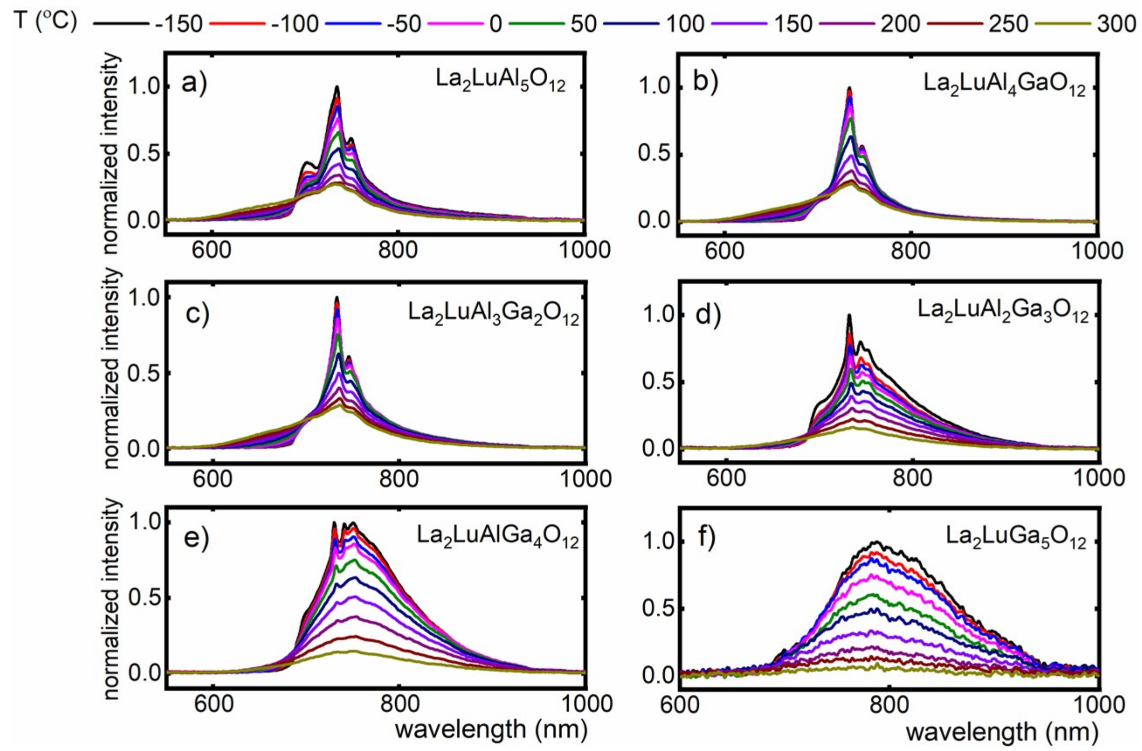


**Figure S.6.** Comparison of $La_2LuAl_{5-y}Ga_yO_{12}$: 1%$Cr^{3+}$ emission spectra in the function of temperature: $La_2LuAl_5O_{12}$ –a); $La_2LuAl_4GaO_{12}$ –b); $La_2LuAl_3Ga_2O_{12}$ –c); $La_2LuAl_2Ga_3O_{12}$ -d); $La_2LuAlGa_4O_{12}$ –e); $La_2LuGa_5O_{12}$ –f).

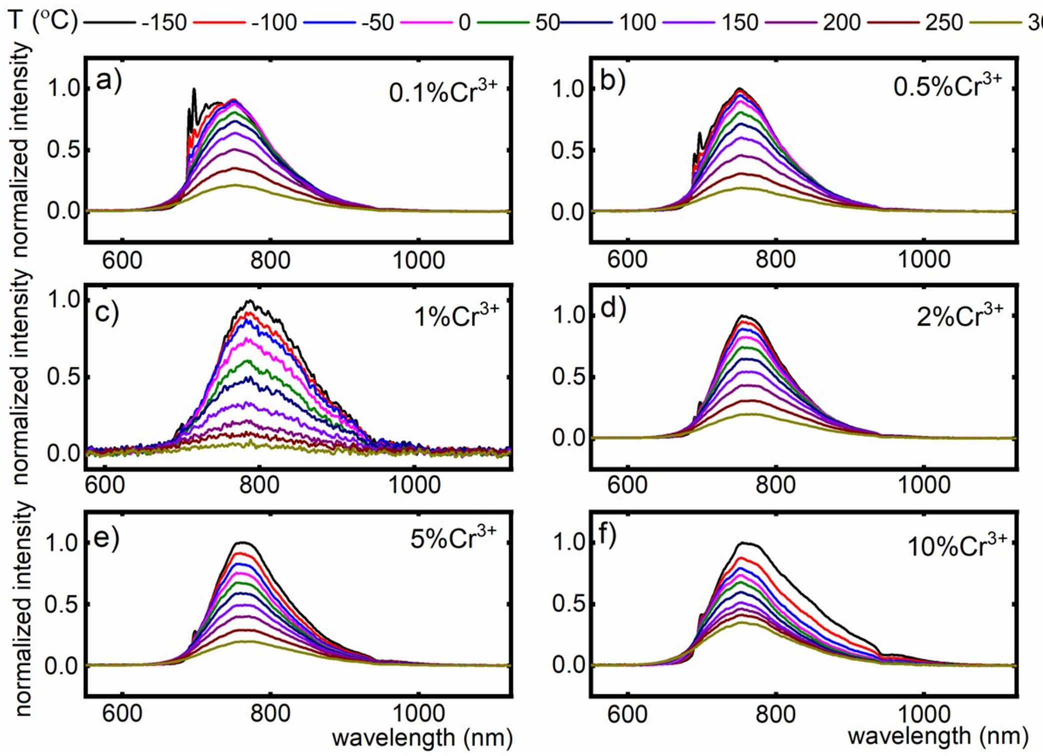


**Figure S.7.** Comparison of $La_2LuGa_5O_{12}$: %$Cr^{3+}$ emission spectra in the function of temperature with different concentration of $Cr^{3+}$ dopant: 0.1%$Cr^{3+}$ –a); 0.5%$Cr^{3+}$ –b); 1%$Cr^{3+}$ –c); 2%$Cr^{3+}$ –d) 5%$Cr^{3+}$ –e); 10%$Cr^{3+}$ –f).

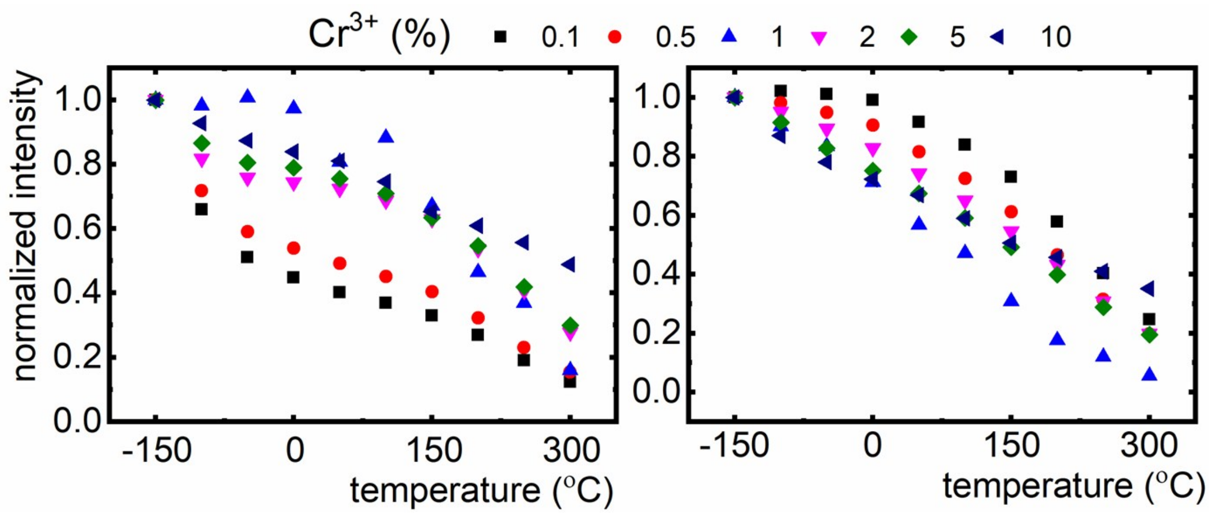


**Figure S.8.** Integral intensity of $^2E \rightarrow ^4A_2$ -a) and $^4T_2 \rightarrow ^4A_2$ -b) electronic transitions for different $Cr^{3+}$ concentrations in the function of temperature for $La_2LuGa_5O_{12}$:%$Cr^{3+}$.

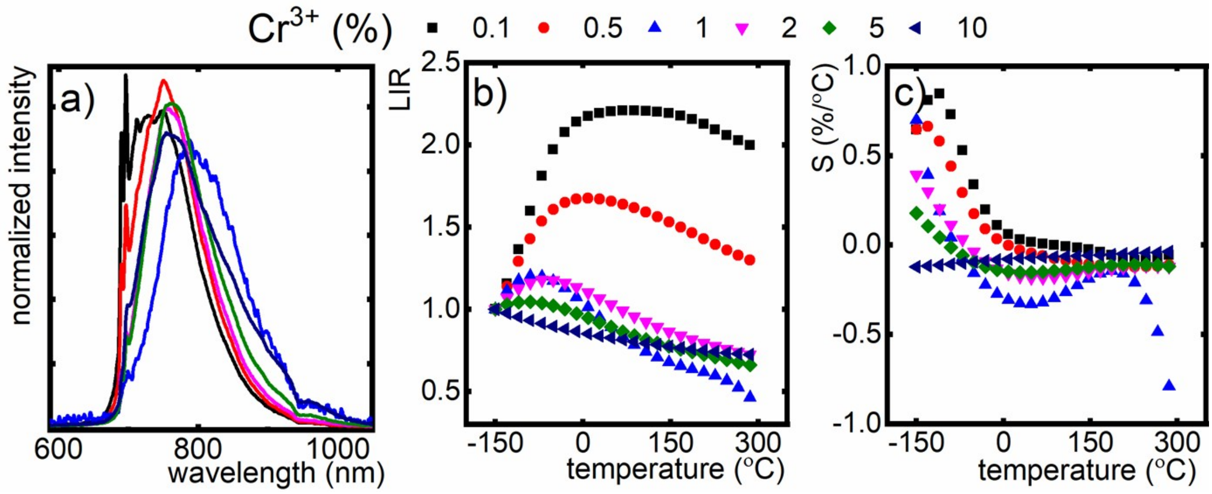


**Figure S.9.** Comparison of $La_2LuGa_5O_{12}$: %$Cr^{3+}$ emission spectra with different concentration of $Cr^{3+}$ dopant, measured at -150°C –a); evolution of $^4T_2 \rightarrow ^4A_2/^2E \rightarrow ^4A_2$ luminescence intensity ratio (LIR) –b) with the corresponding sensitivities –c) in the function of temperature.

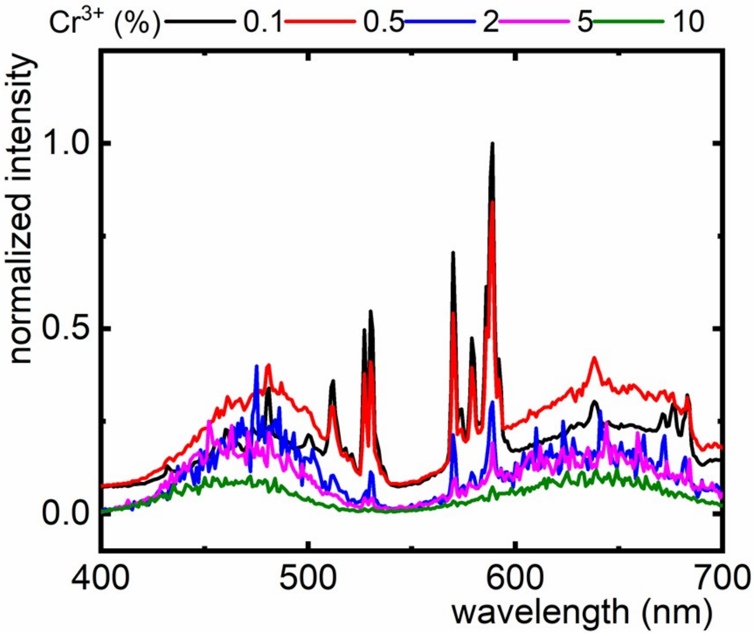


**Figure S.10.** Comparison of $La_2LuGa_5O_{12}$: $\%Cr^{3+}$,$1\%Nd^{3+}$ excitation spectra with different concentration of $Cr^{3+}$ dopant, obtained in temperature 77K.

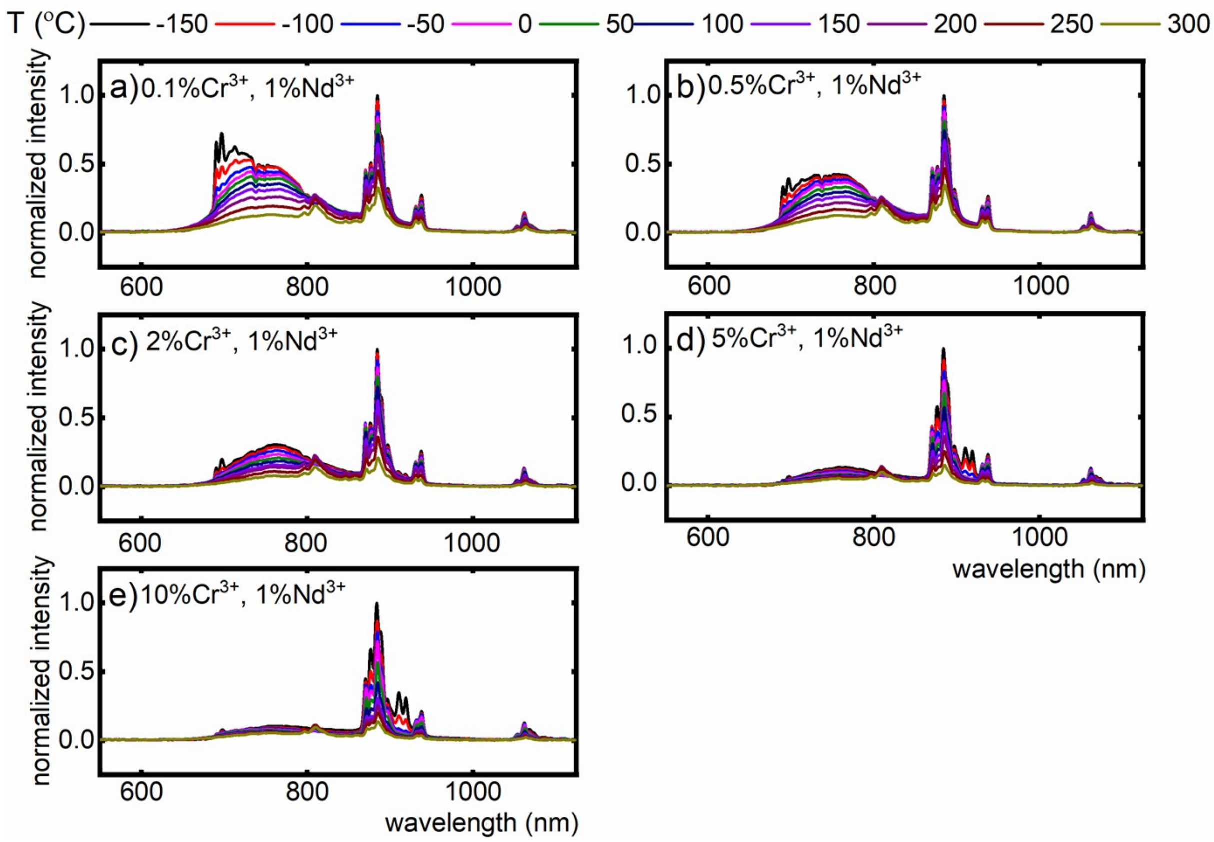


**Figure S.11.** Comparison of $La_2LuGa_5O_{12}$: $\%Cr^{3+}$,$1\%Nd^{3+}$ emission spectra in the function of temperature with different concentration of $Cr^{3+}$ dopant: $0.1\%Cr^{3+}$,$1\%Nd^{3+}$ –a); $0.5\%Cr^{3+}$,$1\%Nd^{3+}$ –b); $2\%Cr^{3+}$,$1\%Nd^{3+}$ –c); $5\%Cr^{3+}$,$1\%Nd^{3+}$ –d); $10\%Cr^{3+}$,$1\%Nd^{3+}$ –e) for 450nm excitation line.

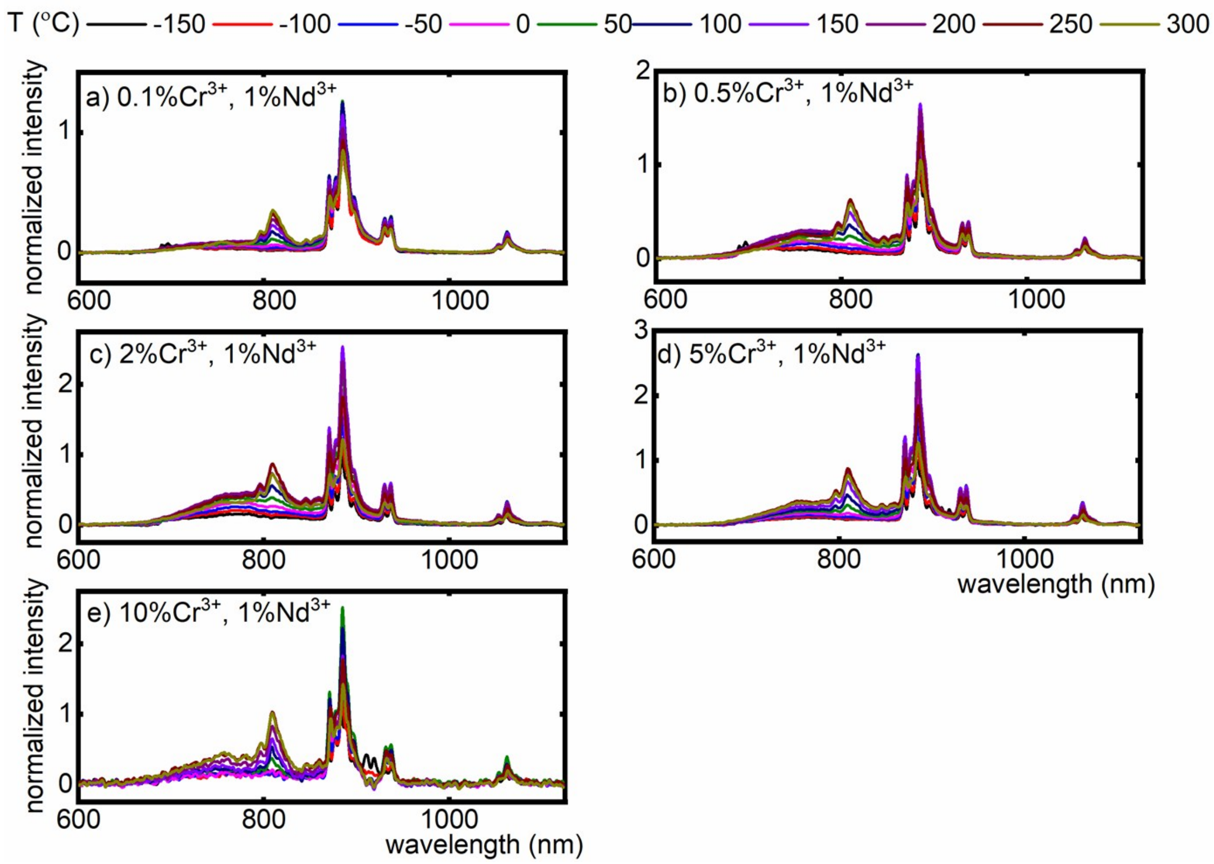


**Figure S.12.** Comparison of $La_2LuGa_5O_{12}$: %$Cr^{3+}$,1%$Nd^{3+}$ emission spectra in the function of temperature with different concentration of $Cr^{3+}$ dopant: 0.1%$Cr^{3+}$,1%$Nd^{3+}$ –a); 0.5%$Cr^{3+}$,1%$Nd^{3+}$ –b); 2%$Cr^{3+}$,1%$Nd^{3+}$ –c); 5%$Cr^{3+}$,1%$Nd^{3+}$ –d); 10%$Cr^{3+}$,1%$Nd^{3+}$ –e) for 532 excitation line.

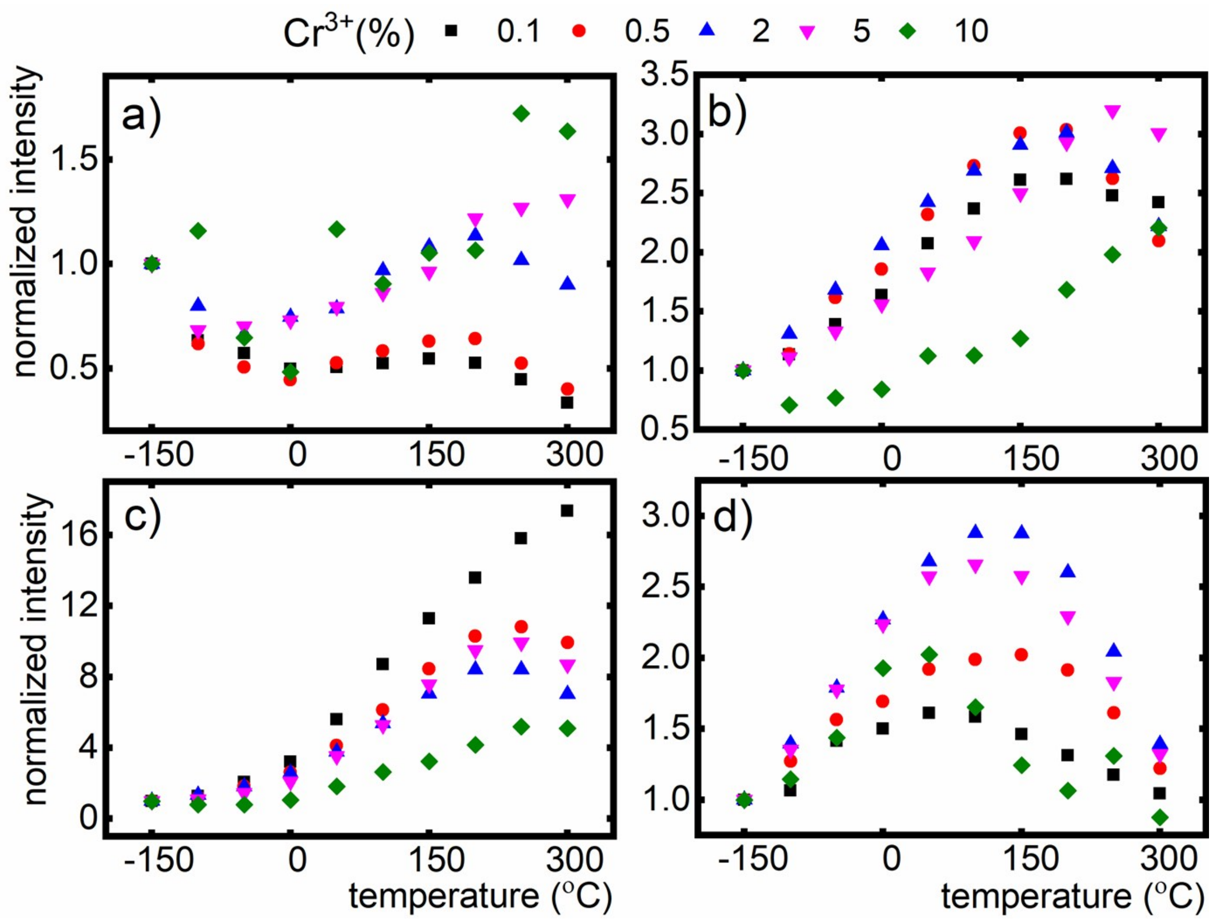


**Figure S.13.** Integral intensity of $^2E \rightarrow ^4A_2$ -a), $^4T_2 \rightarrow ^4A_2$ -b) $^4F_{5/2} \rightarrow ^4I_{9/2}$ -c), $^4F_{3/2} \rightarrow ^4I_{9/2}$ -d) electronic transitions for different $Cr^{3+}$ concentrations in the function of temperature for $La_2LuGa_5O_{12}$:%$Cr^{3+}$, 1%$Nd^{3+}$ (532nm excitation line).

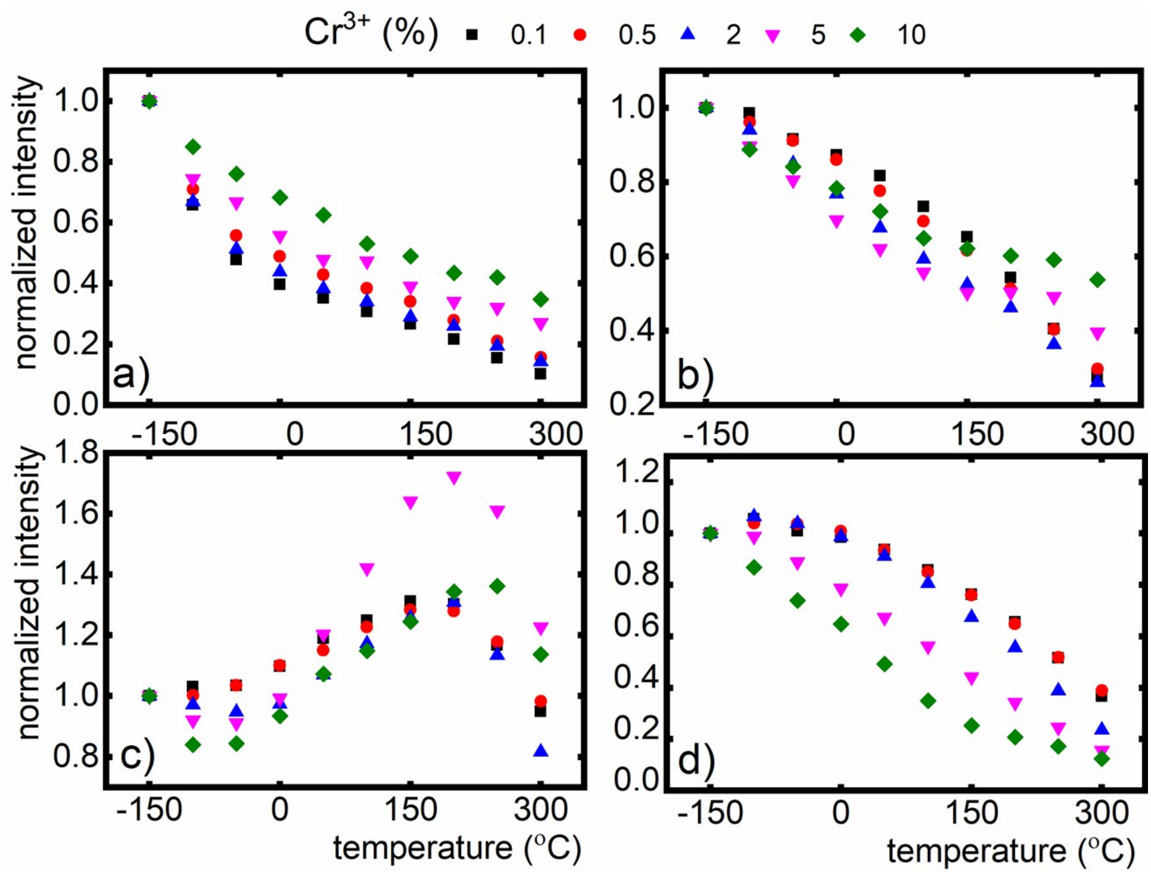


**Figure S.14.** Integral intensity of $^2E \rightarrow {}^4A_2$ -a), $^4T_2 \rightarrow {}^4A_2$ -b) $^4F_{5/2} \rightarrow {}^4I_{9/2}$ -c), $^4F_{3/2} \rightarrow {}^4I_{9/2}$ -d) electronic transitions for different $Cr^{3+}$ concentrations in the function of temperature for $La_2LuGa_5O_{12}$:%$Cr^{3+}$, 1%$Nd^{3+}$ (450nm excitation line).

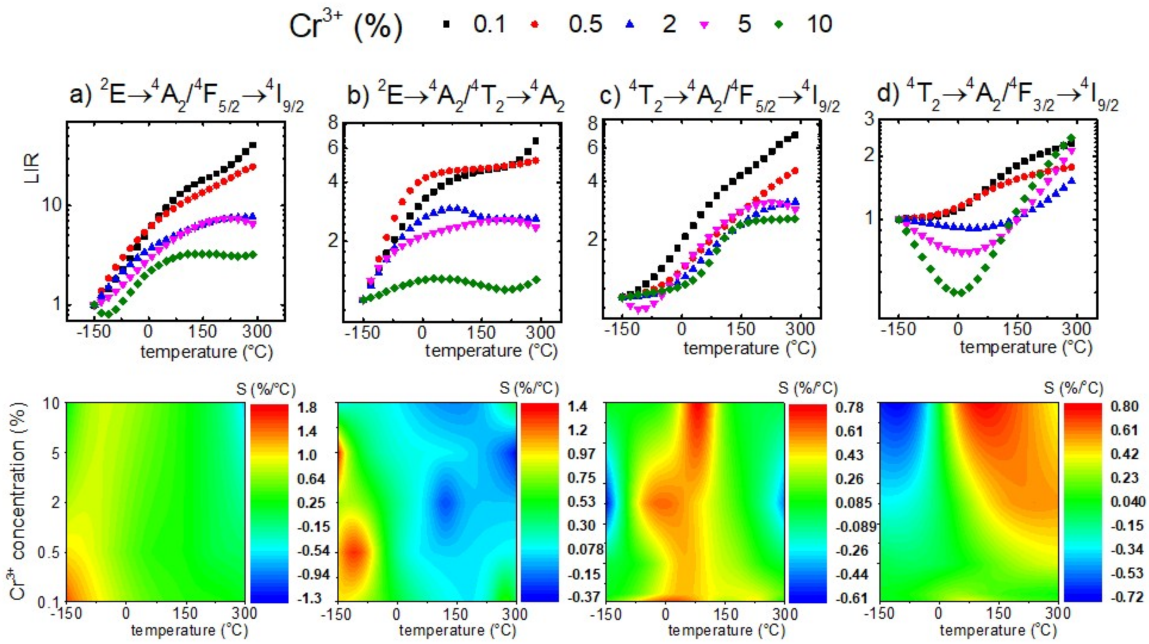


**Figure S.15.** Comparison of $LIR_1$-$LIR_4$ evolution with the corresponding relative sensitivities ($S_1$-$S_4$) in the function of temperature –a-d) for $La_2LuGa_5O_{12}$:%$Cr^{3+}$, 1%$Nd^{3+}$ (532nm excitation line).

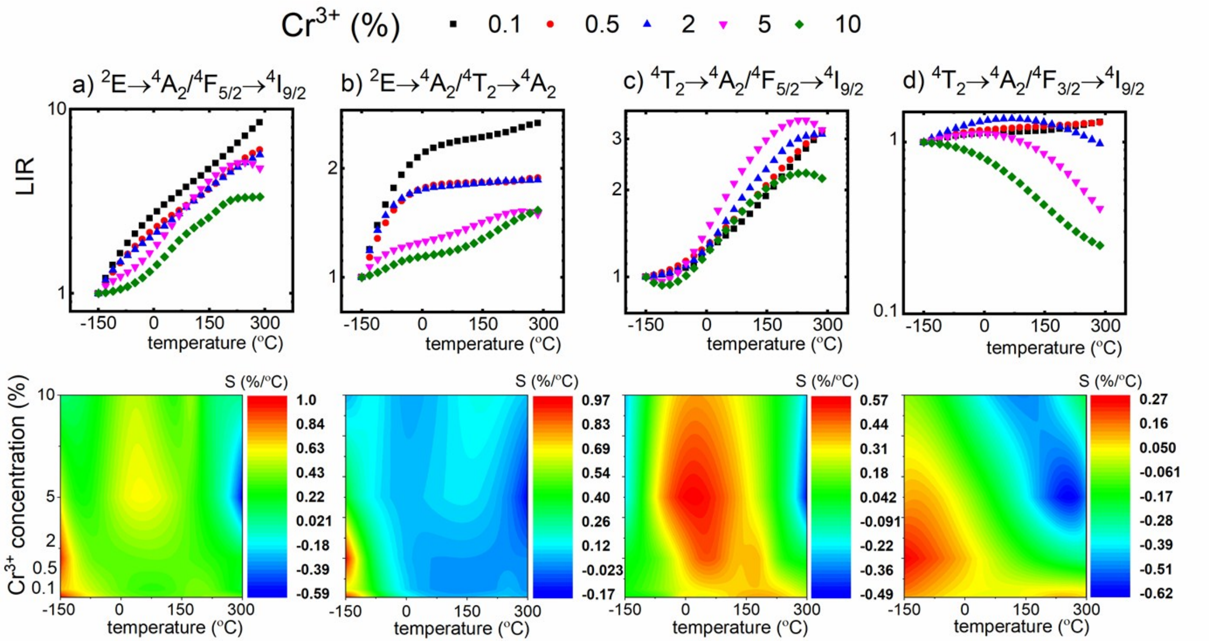


**Figure S.16.** Comparison of $LIR_1$-$LIR_4$ evolution with the corresponding relative sensitivities ($S_1$-$S_4$) in the function of temperature –a-d) for $La_2LuGa_5O_{12}$:%$Cr^{3+}$, 1%$Nd^{3+}$ (450nm excitation line).

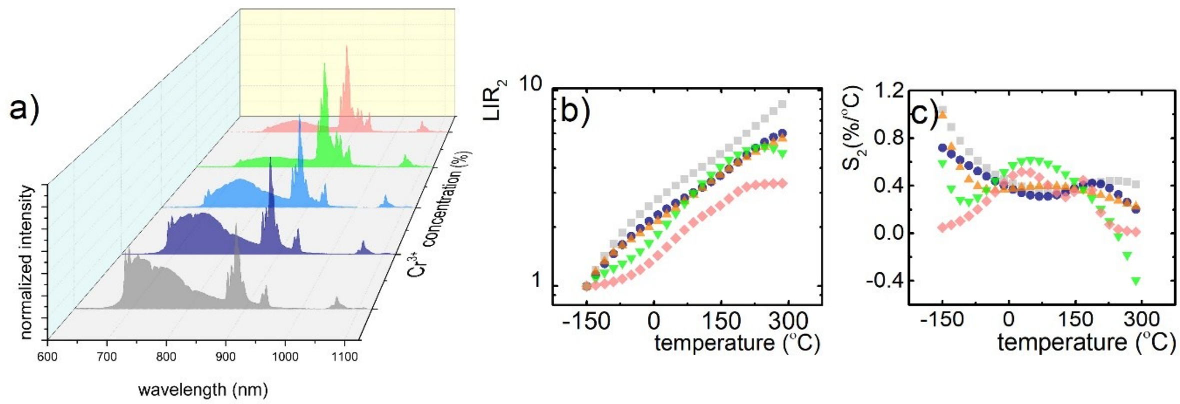


**Figure S.17.** Comparison of emission spectra evolution in the function of $Cr^{3+}$ concentration for $La_2LuGa_5O_{12}$:%$Cr^{3+}$, 1%$Nd^{3+}$, obtained by 450 nm excitation line –a); evolution of $LIR_2$ –b) with the corresponding relative sensitivities ($S_2$) –c) in the function of temperature.

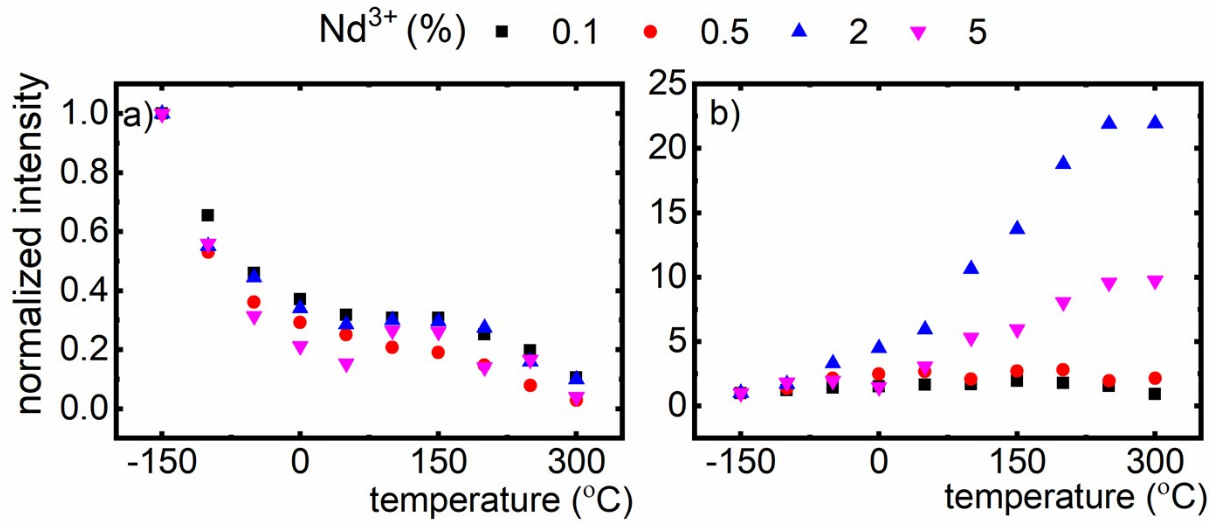


**Figure S.18.** Integral intensity of ${}^4T_2 \rightarrow {}^4A_2$ -a) and ${}^4F_{5/2} \rightarrow {}^4I_{9/2}$ -b) electronic transitions for different $Nd^{3+}$ concentrations in the function of temperature for $La_2LuGa_5O_{12}$:0.5%$Cr^{3+}$, x%$Nd^{3+}$ (532nm excitation line).

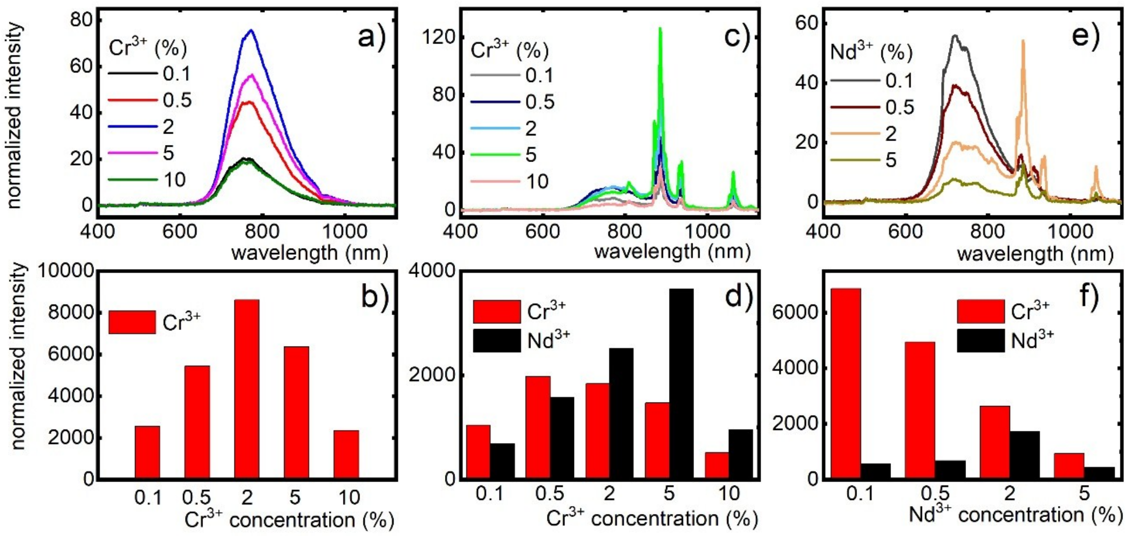


**Figure S.19.** Comparison of $La_2LuGa_5O_{12}$: %$Cr^{3+}$ emission spectra measured for the same experimental conditions –a) and integral emission intensity –b) in the function of $Cr^{3+}$ concentration. Comparison of $La_2LuGa_5O_{12}$: %$Cr^{3+}$,1%$Nd^{3+}$ emission spectra –c) and integral emission intensity –d) in the function of $Cr^{3+}$ concentration. Comparison of $La_2LuGa_5O_{12}$: 1%$Cr^{3+}$,x%$Nd^{3+}$ emission spectra –e) and integral emission intensity –f) in the function of $Nd^{3+}$ concentration. (All presented emission spectra were obtained at room temperature with the use of 445nm excitation line.)

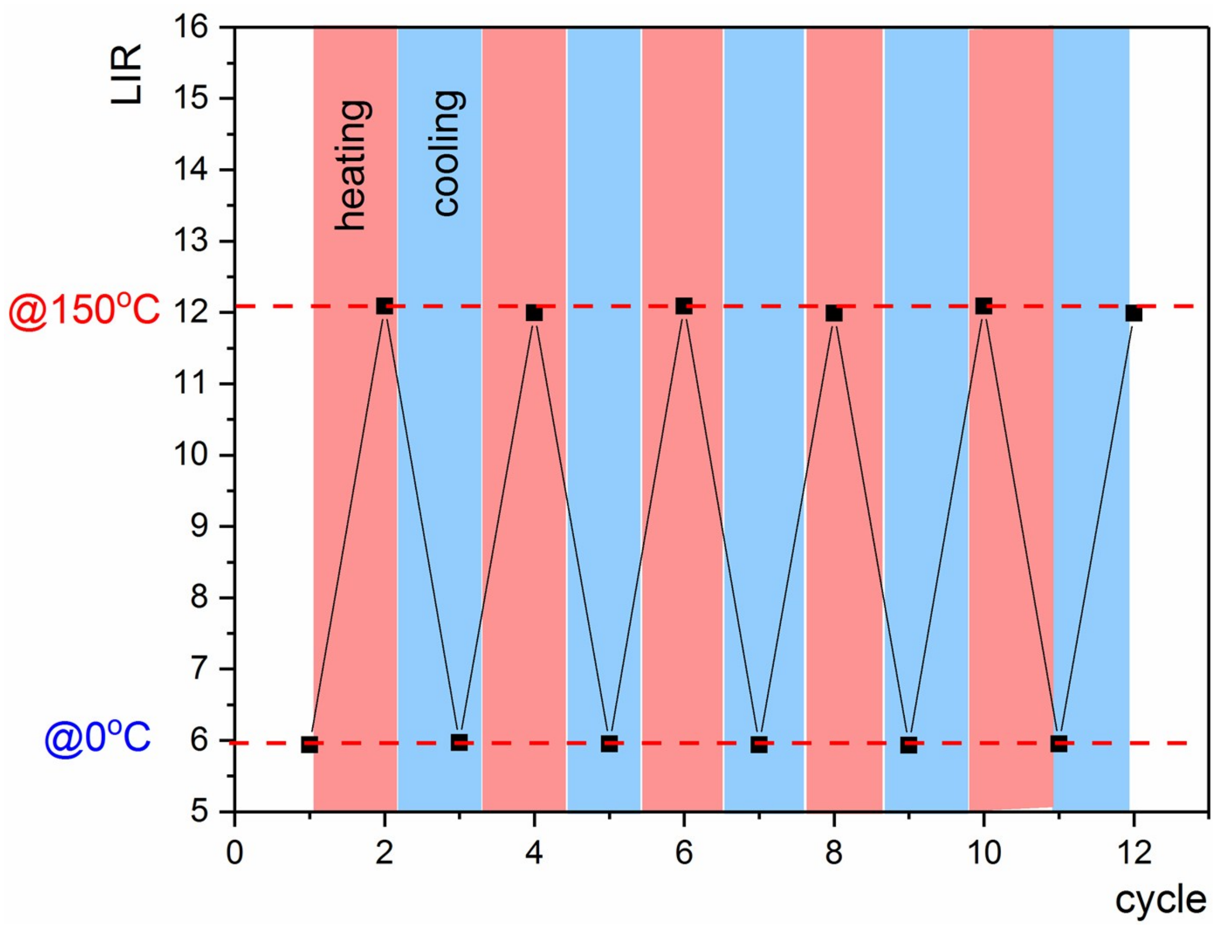


**Figure S.20** The reproducibility of temperature readout using $La_2LuGa_5O_{12}$:1%$Cr^{3+}$, 5%$Nd^{3+}$ nanocrystals verified within the framework of 12 heating-cooling cycles